J Nanostruct 14(1): 295-310, Winter 2024

RESEARCH PAPER

Removal of Malachite Green Dye by Adsorption over the Synthesized Composites of Iron Oxide and Nickel Oxide Nanoparticles

Alaa Salman Hussein [1,2]*, *Abbas Jasim Atiyah* [1]

[1] College of Sciences, Department of Chemistry, University of Babylon, Iraq

[2] College of Dentistry, Department of Basic Sciences, University of Babylon, Iraq

ARTICLE INFO

Article History:
Received 19 October 2023
Accepted 27 December 2023
Published 01 January 2024

Keywords:
Adsorption processes
Iron oxide
Malachite Green dye
Nickel oxide

ABSTRACT

The current study involves synthesis of iron oxide, nickel oxide and then synthesis of FeO-NiO composites in three different ratios (1:1, 1:2, and 2:1). These materials were synthesized using co-precipitation method. The synthesized above materials were characterized by using different analytical and spectroscopic methods such as X-ray diffraction technique (XRD), scanning electron microscopy (SEM-EDX), specific surface area (BET), and Fourier transform infrared spectroscopy (FTIR). The activity of these synthesized materials was investigated by removing of Malachite Green (MG) dye from its aqueous solution by adsorption over these materials. Different adsorption conditions and parameters were conducted such as mass of catalyst, concentration of the used dye, pH of the solution and the effect adsorption temperature. From the obtained results, the best ratio of FeO-NiO composites was (2:1) which exhibited best removal efficiency of the used dye over this composite and it was around 96%, and this was obtained over using 0.20 g. of catalyst, 20 ppm of Malachite Green dye, 6 pH and 25 °C. Adsorption isotherm was investigated for adsorption of MG dye over FeO-NiO composites (2:1), and the obtained results showed that it was more fitted with Freundlich isotherm. Also, the activation energy was calculated applying Arrhenius equation for this adsorption and it was around 15 KJ/mol., which falls in the range of physical adsorption.

How to cite this article
Hussein A., Atiyah A. Removal of Malachite Green Dye by Adsorption over the Synthesized Composites of Iron Oxide and Nickel Oxide Nanoparticles. J Nanostruct, 2024; 14(1):295-310. DOI: 10.22052/JNS.2024.01.030

INTRODUCTION

In the last few decades, and as a result of massive growth in population over the world, this was accompanied with high consumption of industrial materials including food industry, pharmaceutical industry, pesticides industry, textile industry, and oil refinement processes. All these activities were increased significantly, which leads to high levels of pollution in our environment including air, water and soil. Therefore, particularly in the chemical industries, there is a need for efficient and effective procedures to remove or at least control on the levels of the environmental pollution at the safe limit [1-3]. In this context, wastewaters refer to water that has been contaminated by excess substances that detract from its quality and render it unfit for human consumption as well as for many industrial processes. Wastewater varies greatly

* Corresponding Author Email: alaa.allabban@gmail.com

in composition and is very reliant on the original point of its origin. Wastewater typically contains inorganic compounds, such as solutes, heavy metals, metal ions, and metal sulphides [4]. Dyes compounds are used to provide a desired color to a variety of materials, including fibers, textiles, leather, paint, pigment and paper and many other purposes especially in our modern life [5]. In this way, at least one hundred thousand distinct dye categories are presently available, and they play an important role in the textile, paint, and pigment production sectors. It is estimated that every year, 1.6 million tons of dyes are generated to supply the industrial sector, with 10 – 15% of this amount being discharged as wastewater [6]. Currently, wastewaters that contain dyes and heavy metals can be treated using a variety of techniques, such as adsorption, precipitation, membrane filtration, chemical oxidation, ion exchange, and the electrolytic process. Most methods, however, are prohibitively expensive, time-consuming, and problematic when it comes to waste management. Among these methods, adsorption processes seem to be a promising technique [7]. In the last few years, a big rise in the synthesis of magnetic adsorbent materials nanoparticles of Fe, Co, and Ni due to their superior magnetic characteristics and prospective applications in a wide variety of applications, such as catalysis, memory storage devices, and sensors. Magnets have several medical applications, including magnetic resonance imaging and the hyperthermia therapy of cancer cells [8].

Iron oxides are chemicals formed when iron and oxygen react chemically; thus far, scientists have found about 16 different iron oxides. Rust is a naturally occurring type of iron (III) oxide. Magnetite (Fe_3O_4), magnetite (γ-Fe_2O_3), and hematite (α-Fe_2O_3) are the three most frequent iron oxides form in nature. The scientific and technological fields both rely heavily on these oxides [9, 10].

Malachite green (MG) dye is a green crystalline powder that dissolves in water and is a soluble organic cationic dye [11]. Malachite Green, also known as Leucomalachite Green, has the chemical formula $C_{23}H_{26}N_2O$ and occurs in many different forms. Among these is its usage as an industrial dye in the tanning and coloring of leather, silk, paper, plastic, and other materials. It is present in the waste products of these businesses and must be eliminated in various ways [12]. Malachite green and leucomalachite green structures and their conversions are shown in Fig. 1 [13].

The current study aims to synthesize of composites of FeO-NiO in three different ratios. Then the activity of these materials would be investigated by following removal of MG dye from its aqueous solution by adsorption over these materials. This also would involve screening different conditions and factors that can effect on the adsorption efficiency.

MATERIALS AND METHODS

Used chemicals and materials

Iron (II) chloride tetrahydrate [$FeCl_2.4H_2O$] was obtained from (CDH) with assay 97%, ferric chloride anhydrous [$FeCl_3$] from (CDH) with assay 97%, ferric nitrate nonahydrate [$Fe(NO_3)_3.9H_2O$] was obtained from (THOMAS BAKER) with assay 98%, nickel (II) nitrate hexahydrate [$Ni(NO_3)_2.6H_2O$] was obtained from (CDH) with assay 99%, sodium

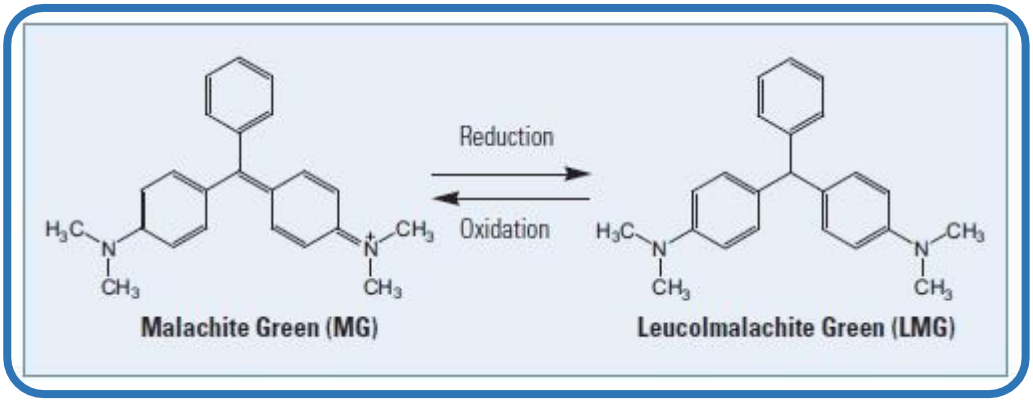

Fig. 1. Structure and conversion of Malachite Green dye and Leucomalachite Green

carbonate [Na_2CO_3] was obtained from (VWR INTERNATIONAL) with purity 99.9%, hydrochloric acid [HCl] was obtained from (BDH) with 37% and Malachite Green (MG) dye [$C_{23}H_{26}N_2O$], M.W. 346.46 mol.g^{-1} was obtained from (BDH) with dye content 99%.

Synthesis of iron oxide

In this part, the co-precipitation method was applied to synthesize iron oxide nanoparticles. This technique is the most ideal traditional approach for manufacturing iron oxide nanoparticles because of its non-toxic solvent, high yield, and ease of repeatability [14]. According to this method, 0.7954g. of iron (II) chloride, $FeCl_2.4H_2O$, and 1.2974 g. of iron (III) chloride, $FeCl_3$ were dissolved in distilled water. Throughout the experiment, the mole ratio of iron (II) chloride to iron (III) chloride was held constant at 1:2. After that, the solution was stirred for 30 minutes on a hot plate using a magnetic stirrer (Heidolph MR Hei-Standard). Different processing temperatures, pH, and stirring speeds were all controlled throughout mixing processes. The combined solution was then separated by centrifugation at 4000 rpm for 15 minutes. The obtained solid precipitate was dried in an oven at 100 °C for 24 hours. Finally, using a pestle and mortar, the dried dark brown obtained samples were collected and crushed into powder form. Equation 1-3 depicts the chemical balancing equation for the reaction $FeCl_2.4H_2O$ and $FeCl_3$, where γ-Fe_2O_3 was the end product and water was the by-product [15]:

$$Fe^{2+} + 2Fe^{3+} + 8OH^- \longrightarrow Fe_3O_4 + 4H_2O \quad (1)$$

$$Fe_3O_4 + 0.25O_2 + 4.5H_2O \longrightarrow 3\mathrm{Fe}(OH)_3 \quad (2)$$

$$2\mathrm{Fe}(OH)_3 \longrightarrow \gamma Fe_2O_3 + 3H_2O \quad (3)$$

Synthesis a composite of iron oxide – nickel oxide

The co-precipitation method was utilized to synthesize the supported co-catalyst. This process was conducted using mixture of $Ni(NO_3)_2.6H_2O$ and $Fe(NO_3)_3.9H_2O$ (in a ratio of 1:1, 1:2 and 2:1). This mixture was dissolved in 400 ml of deionized distilled water at a constant stirring and under ambient atmospheric conditions. A digital pH meter was used to adjust the pH of the final combination to the specified level. The solution was maintained at a temperature of (70–75) ℃ while Na_2CO_3 (1M) was added drop by drop as a precipitating agent. The resulting solution's pH was controlled to remain in the 9.0–9.1 range. Then the resulted mixture was kept undisturbed for 2 hours at room temperature with a constant stirring. A

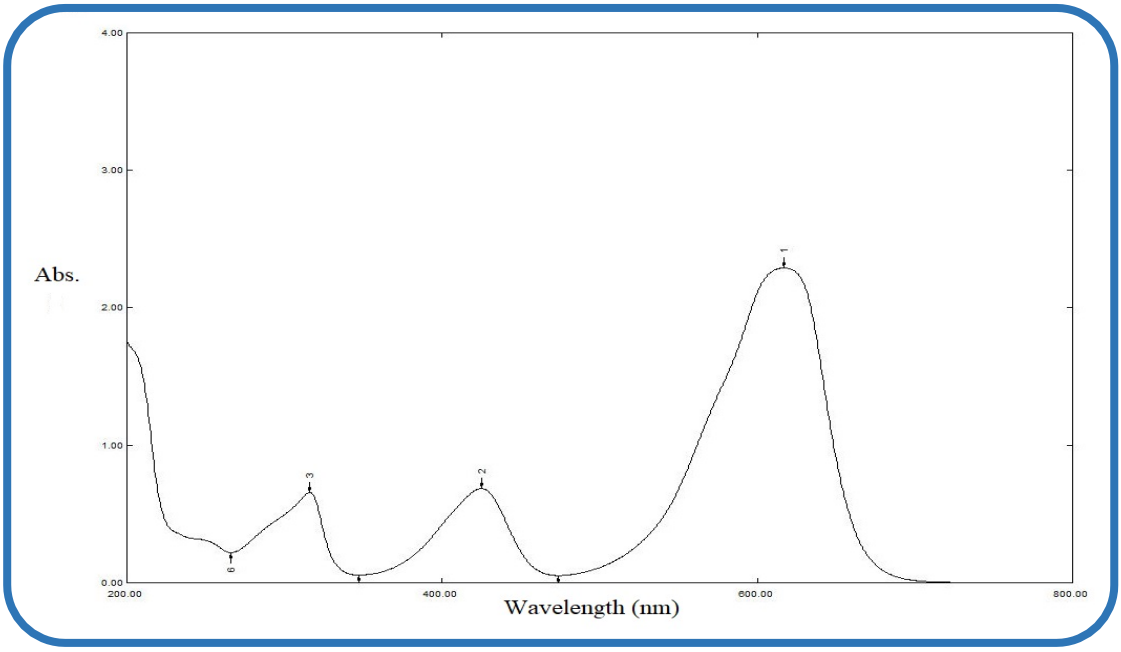

Fig. 2. UV. Vis. Spectrum of (20 ppm) MG dye, λmax 617 nm.

Buchner filtration flask equipped with a vacuum pump was used to remove the contaminants from the resulting combination. After that, the material was calcined at 500℃ for 4 hours at a heating rate of 100 ℃ per minute in an air environment [16].

Adsorption study

Adsorption study involves investigation of the optimal conditions for the removal of MG dye from its aqueous solution by adsorption over the synthesized catalysts (neat iron oxide and a composite of iron oxide / nickel oxide). In this part, adsorption experiments were conducted in a closed system of the glass dual wall reactor kind, with a chiller (Julabo model EH/Germany) serving as the temperature controller. The reaction mixture was agitated using a magnetic stirrer (Heidolph MR Hei-Standard).

In each run, MG dye solution (20 ppm, 100 ml) was suspended over 0.20 g. of the used catalysts. Periodically, samples (2) ml were withdrawn every 15 minute and then centrifuged carefully using (80-1 Electric Centrifuge). Then the absorbance of the supernatant liquids was recorded at a wavelength of 617nm using a SHIMADZU spectrophotometer double beam (UVProbe). The adsorption time was 60 minutes. The efficiency of MG dye removal (R%) was calculated using the following equation:

$$\text{Removal } \% = \frac{(C_\circ - C_t)}{C_\circ} \times 100 \quad (4)$$

Where C_0 and C_t are the concentrations values at time zero and time t, respectively [17]. UV. Vis. Spectrum of MG dye is shown in Fig. 2 to obtain λmax of dye (617 nm). Fig. 3 shows a calibration curve of MG dye in the range of concentrations from 1 to 25 ppm.

RESULTS AND DISCUSSION

Characterization of the prepared materials

X–Ray Diffraction (XRD) of the synthesized materials

Crystal morphology of the synthesized materials was investigated using XRD technique. XRD patterns were conducted using PANlytical X- -rays diffraction with CuK radiation (1.542 A, 40 KV, 30 MA), in the range of 2Θ = 10-80º using a Shimadzu XRD6000 - Japan. Fig. 4 illustrates XRD patterns of four samples of iron oxide and it's composite with nickel oxide (FeO, and FeO-NiO in three different ratios, 1:1, 1:2 and 2:1). These patterns of iron oxide are showed some characteristic peaks of this oxide at 2Θ = (24.24), (33.21), (35.7), (40.95), (49.55), (54.11), (62.45) and (64.03) and these are corresponded to the planes (012), (104), (110),

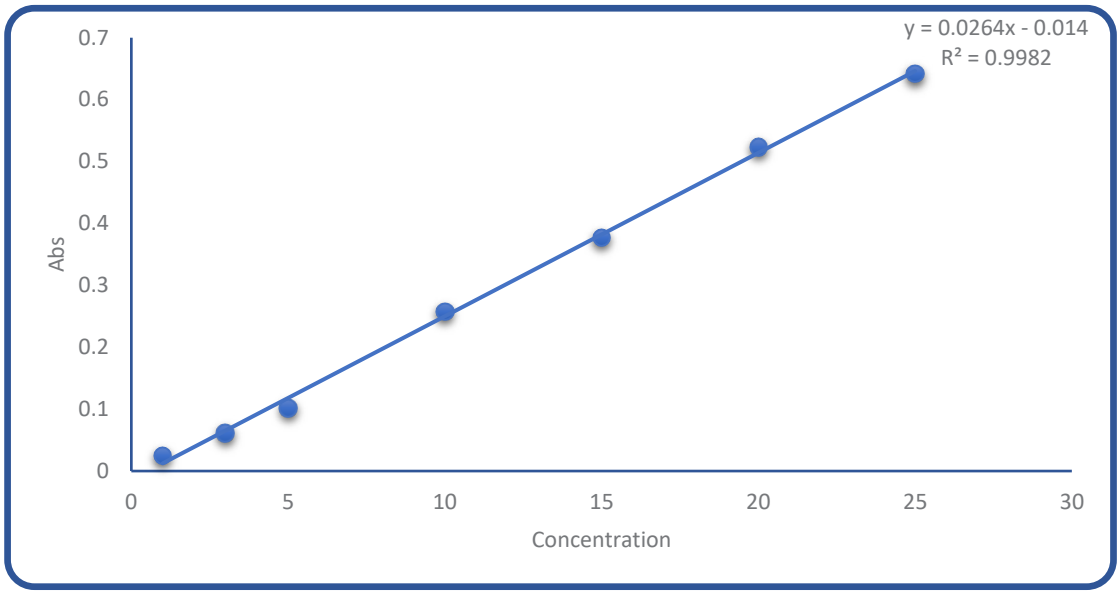

Fig. 3. Calibration curve of MG dye (1 – 25) ppm.

(113), (024), (116), (214) and (300) respectively assigned to the direction planes of rhombohedra structure of α-Fe_2O_3 phase (JCPDS card No: 79 – 0007) [18]. The other patterns of composites of iron oxide with nickel oxide are showed some diffraction peaks at 2Θ = (35.84), (43.456), (63.03) and (75.41), these are corresponded to the planes (111), (200), (220) and (311) respectively. These peaks are almost agree with the standard patterns of nickel oxide nanoparticles (JCPDS, 78 – 0643) [19]. The size of crystallite can be calculated applying Scherer's equation, $D = k \lambda / \beta \cos\vartheta$ where the constant k is taken to be 0.94, λ is the wavelength of respectively [20]. From the obtained results, the crystallite sizes were around 21 nm for FeO, and 30 nm for FeO-NiO (1:1), 24 nm for FeO-NiO (1:2) and 16 nm for FeO-NiO (2:1). So that, all the synthesized materials in the present study are full in nanometer scale.

Fourier Transform Infrared Spectroscopy (FTIR) for the synthesized materials

FTIR spectra for the synthesized four samples of iron oxide and its composites with nickel oxide are shown in Fig. 5. From these spectra, the peaks at 559.255cm^{-1}, 454.154 cm^{-1}, 545.756cm^{-1} and 441.679 cm^{-1} are due to the formation of iron oxide nanoparticle [21]. In FTIR spectrum of iron oxide and nickel oxide composites vibration bands at 410 cm^{-1} can be assigned to nickel-oxygen stretching vibrations, whereas the bands at 606 and 1056 cm^{-1} are attributed to iron-oxygen stretching vibration modes [22].

Scanning Electron Microscopy (SEM) and Energy Dispersive X-rays (EDX) for the synthesized materials

Surface morphology of the synthesized materials was investigated using SEM technique and the obtained images are shown in Fig. 6. From these images it can be seen that, in all samples a spherical shape for the four samples with relative aggregation for these particles was seen. Besides that, all samples have an average particle size to in the range from 23nm to 67nm.

Fig. 7, A, B, C, and D shows EDX results for the

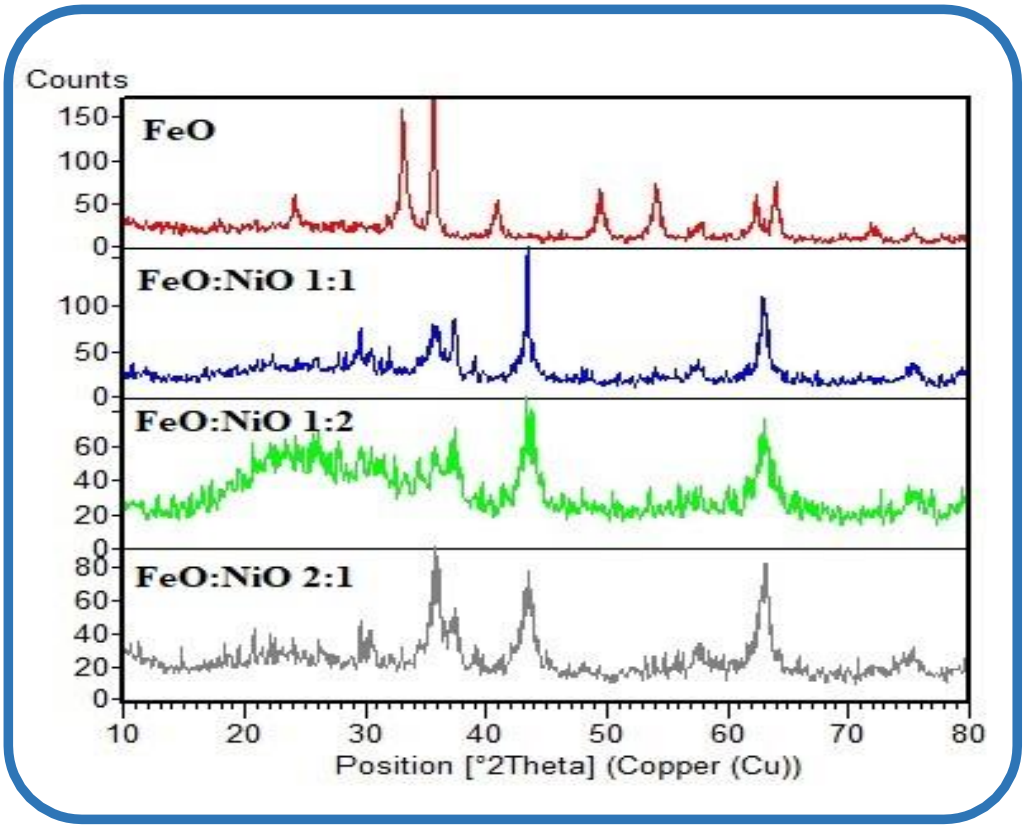

Fig. 4. XRD patterns for neat iron oxide and its composites with nickel oxide

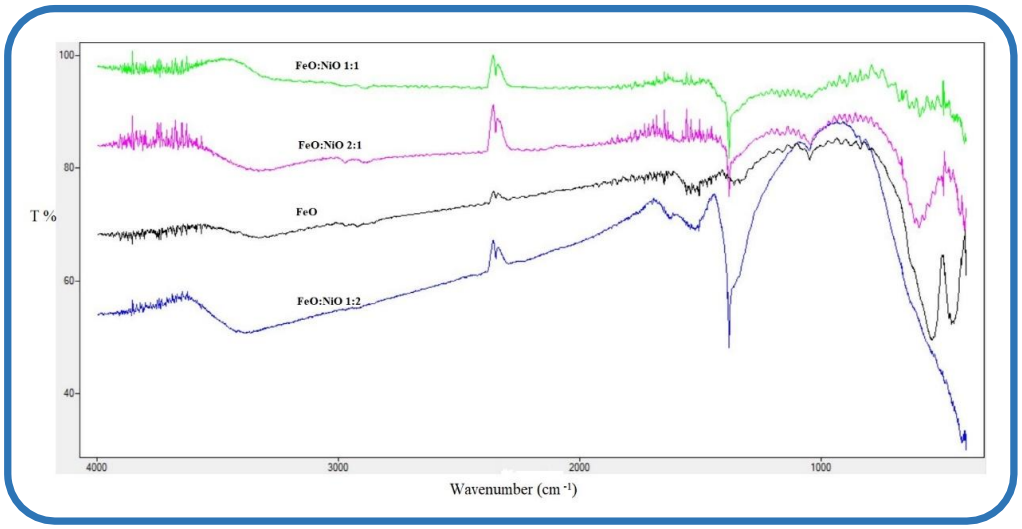

Fig. 5. FTIR specra of iron oxide and its composites with nickel oxide

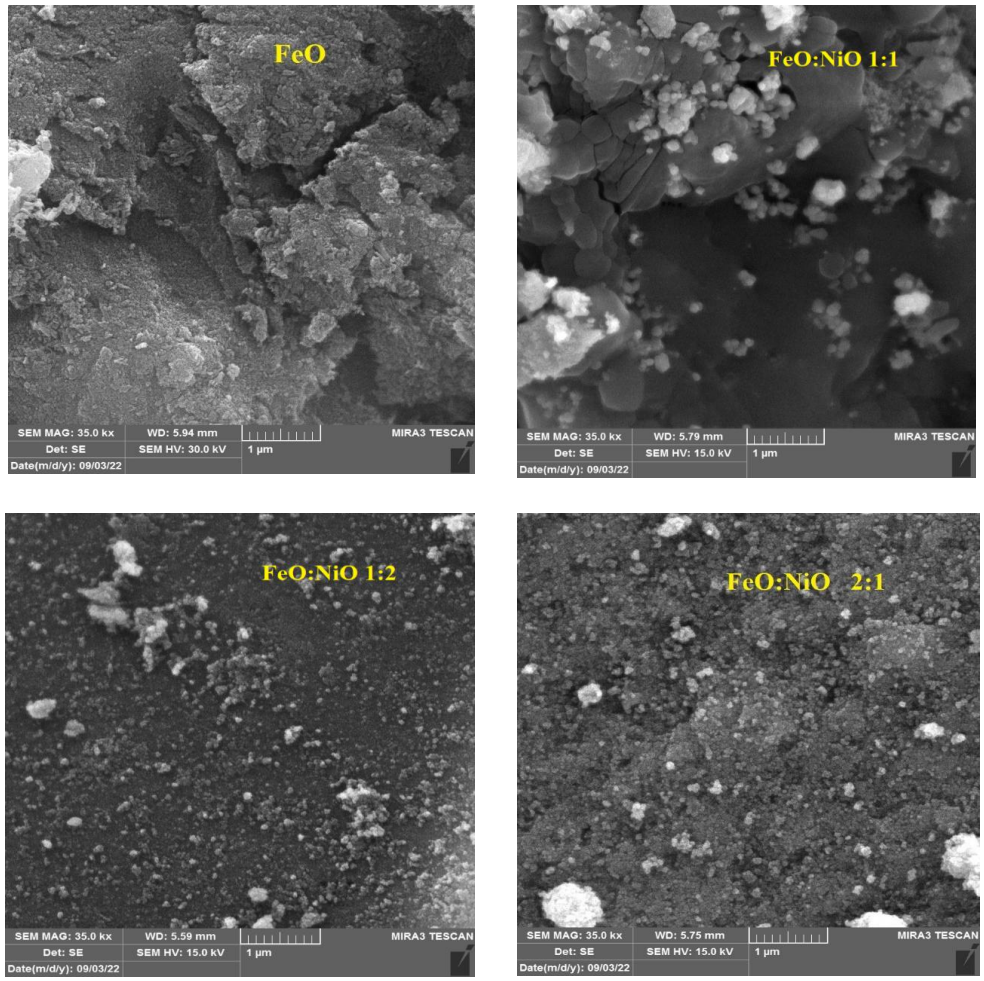

Fig. 6. SEM images of iron oxide and its composites with nickel oxide

synthesized iron oxide aand its composites with nickel oxide neat FeO (A), FeO-NiO(1:1) (B), FeO-NiO (1:2) (C) and FeO-NiO (2:1) (D). These spectra show elemental composition with weight percent

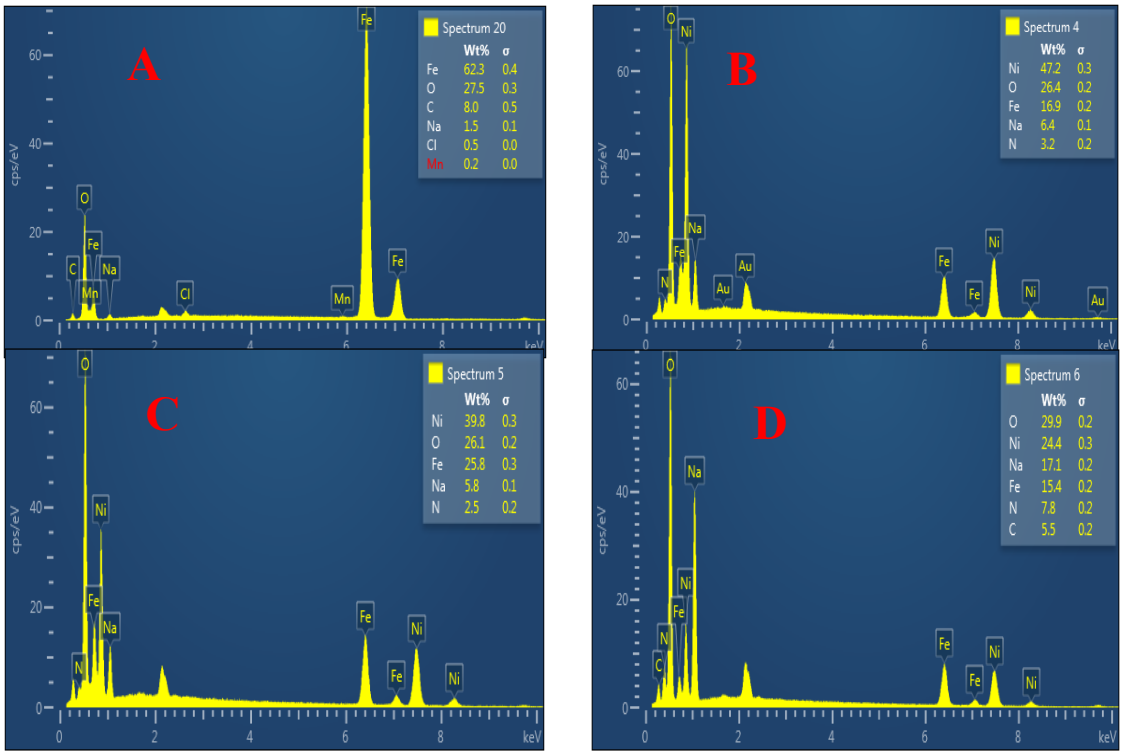

Fig. 7. EDX of iron oxide and co-oxide of iron oxide with nickel oxide

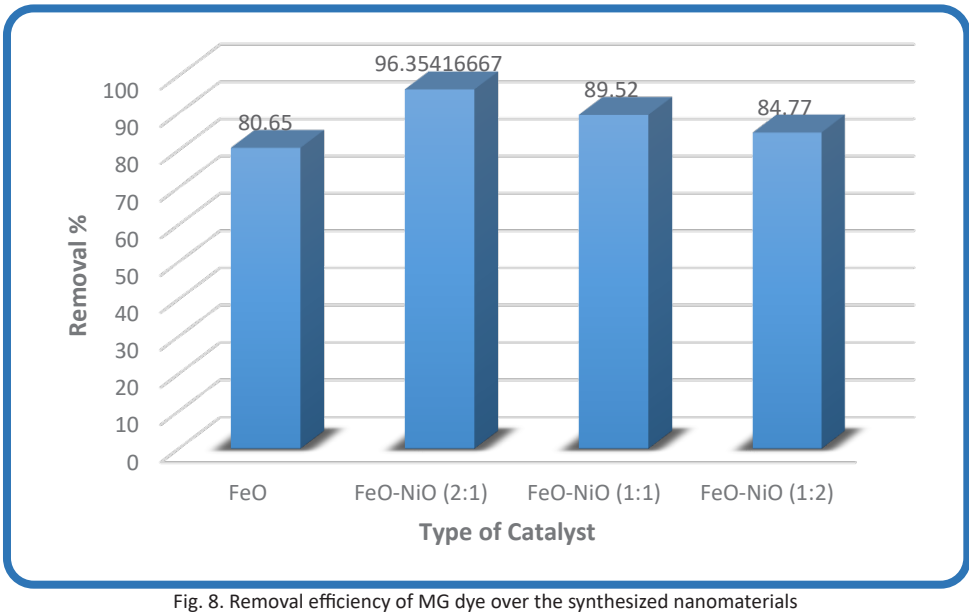

Fig. 8. Removal efficiency of MG dye over the synthesized nanomaterials

of these materials. Fig. 7-A, shows elemental composition of iron oxide, it shows a percent of 62.3 wt% of iron and 27.5 wt% of oxygen, Fig. 7-B, shows elemental composition of a composite of iron and nickel oxide FeO-NiO (1:1), it consists of 47.2 wt% of nickel, 16.9 wt% of iron and 26.4wt% of oxygen. Fig. 7-C, shows elemental composition of a composite of iron and nickel oxide FeO-NiO (1:2), it consists of 39.8 wt% of nickel, 25.8 wt% of iron and 26.1 wt% of oxygen. Fig. 7-D, shows elemental composition of a composite of iron and nickel oxide FeO-NiO (2:1), it consists of 24.4 wt% of nickel, 15.4 wt% of iron and 29.9 wt% of oxygen. In general, these results confirm presence of the proposed element in each sample.

Specific surface areas (BET) for the prepared materials are shown in Table 1. From these results, it can be seen that, there was a reduction in the specific surface area for neat iron oxide in comparison with its composites with nickel oxide in the two ratios (1:1, and 1:2). This probably arises from strong overlap between particles of these two oxides which leads to eliminate of some of active sites at the surface of the resulted composites of these two oxides [23]. On the other, the BET specific surface area for the composite FeO-NiO in a ratio of (2:1), there was an increase in surface area for this composite in comparison with neat iron oxide and other composites in other ratios. This can be attributed to the role of high ratio of iron oxide in this composite to increase porosity of the resulted material which lead to relative increase its specific surface area for this composite [24].

Removal of MG dye by adsorption over the synthesized nanomaterials

To investigate the activity of the synthesized

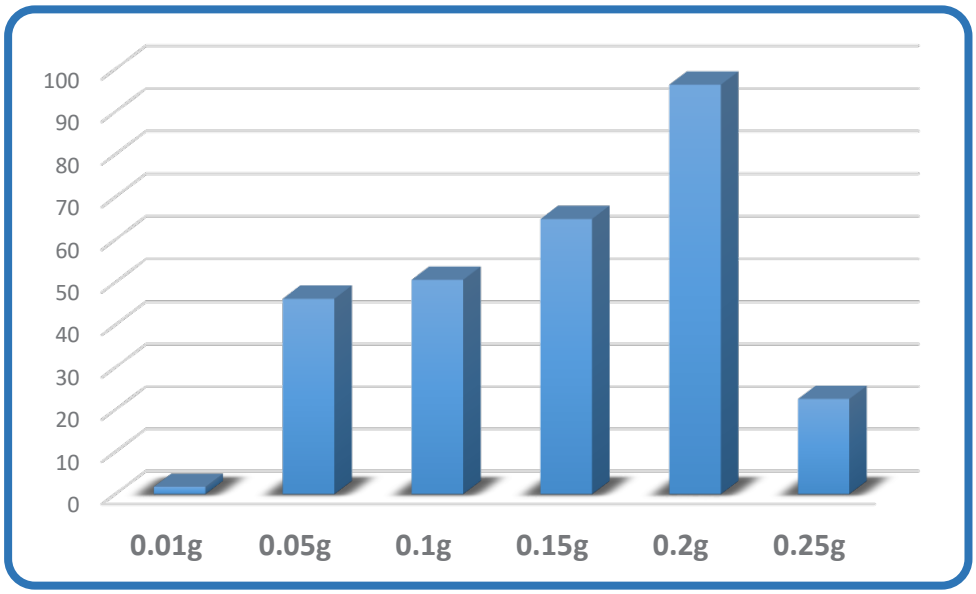

Fig. 9. Effect of using different dosages of FeO-NiO (2:1) on the efficiency of MG removal by adsorption

Table 1. BET surface area and pore size of iron oxide and co-oxide of iron oxide with nickel oxide

Catalysts	BET (m^2 / g)
FeO	47.7045
FeO-NiO 1:1	16.0697
FeO-NiO 1:2	23.6675
FeO-NiO 2:1	59.4898

nanomaterials to be used as adsorbent materials. A series of experiments were conducted using same amount of each one, and some other adsorption conditions including dye concentration, temperature of adsorption, pH of solution, and adsorption period, which was one hour for each run. The obtained results are presented in Fig. 8 that presents removal efficiency for each used material for one hour. From the obtained results, it can be seen that, the optimum removal efficiency was achieved over FeO-NiO (2:1) ratio. This probably arises from its excellent surface properties and its high specific surface area in comparison with other synthesized nanomaterials in different ratios

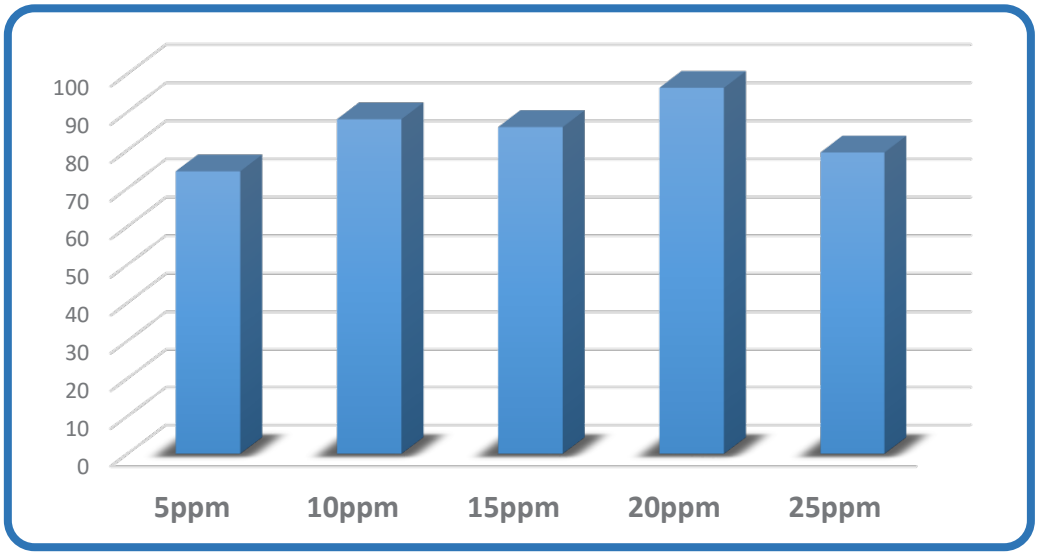

Fig. 10. Effect of MG dye concentration on the efficiency of its removal over FeO-NiO (2:1)

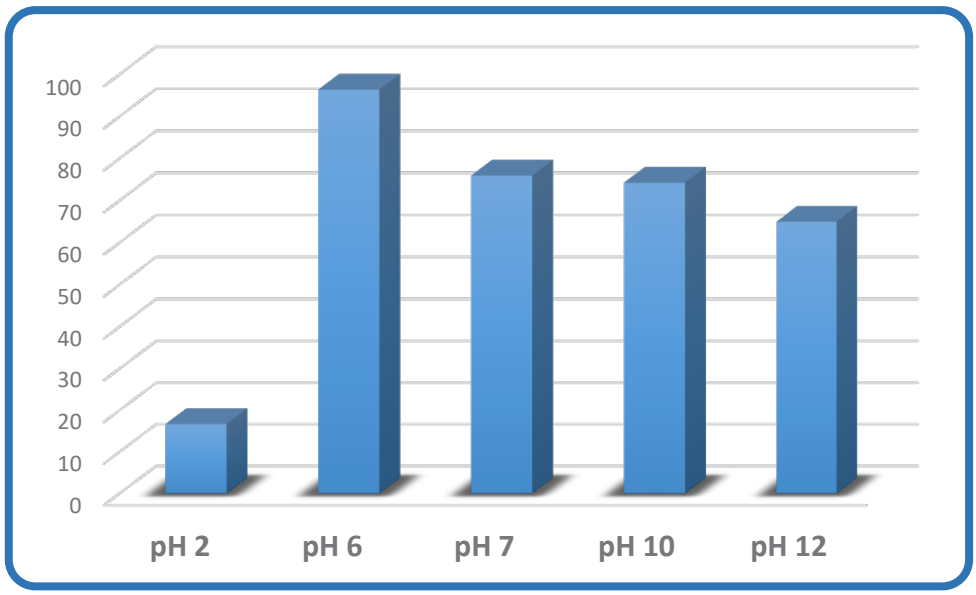

Fig. 11. Effect pH of dye solution on the efficiency of its removal over FeO-NiO (2:1)

[25]. This means that, FeO-NiO ratio (2:1) would be expected to be a best adsorbent among the other synthesized nanomaterials that were synthesized in this study.

Effect dosage of the used adsorbent on the efficiency of MG dye removal

To investigate effect of the used masses of the adsorbent on the efficiency of MG dye removal over the best used adsorbent which was FeO-NiO ratio (2:1). A series of dosages of FeO-NiO ratio (2:1) in the range of 0.01 to 0.25 g. were conducted under a constant of other adsorption parameters for a constant volume and concentration of MG dye. The obtained results are presented in Fig. 9. From the obtained results, it was found that, the best removal efficiency was attained with 0.2 g. of the used adsorbent, and the removal efficiency was increased as the amount of adsorbent was increased. This arises from increase of the available adsorption sites as the amount of the used adsorbent was increased which consequently leads to increase number of dye molecules that can be adsorbed [26]. Upon increasing amount of adsorbent more than 0.2 g., dye adsorption effectiveness was decreased. This probably results from aggregation of the adsorbent particles which leads to reduce the total number of accessible adsorption sites [27]. So that, from the obtained results in this study it was found that, 0.2 g was the optimal dose for in this study which gives a maximum removal efficiency for the used which was around 96%.

Effect of MG dye concentration on the efficiency of its removal over FeO-NiO (2:1) nanomaterial

The effect of dye concentration on the efficiency of its removal by adsorption over FeO-NiO (2:1) was investigated over 0.2 g. of this composite with fixation of all other adsorption conditions with variation MG dye concentration only. To conduct this factor, a series of dye concentrations were investigated from (5 to 25) ppm, over a fixed amount (0.2) g. of the used adsorbent. the remaining concentration of dye after adsorption was recorded according to the previously established calibration curve for the dye. The obtained results are presented in Fig. 10. From these results, it can be seen that, from 5 ppm up to 20 ppm, dye removal efficiency was increased linearly with increase of dye concentration. This can be attributed due to availability of more dye molecules would be present at higher dye concentrations, and these molecules can be adsorbed easily at the unoccupied adsorption sites at the surface of the used adsorbent. After this point, dye concentrations more than (20 ppm), dye removal efficiency was diminished linearly with

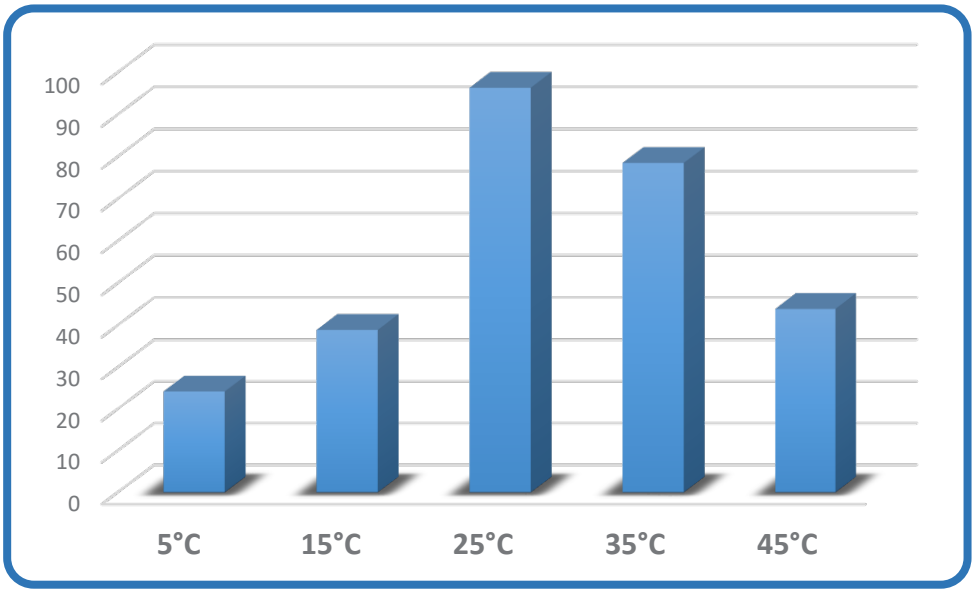

Fig. 12. Effect of temperature on the efficiency of removal of MG dye over FeO-NiO (2:1)

increasing of dye concentrations above this value. This probably arises from numerous additional dye molecules competing for the same amount of adsorption sites due to high dye concentration upon this addition. Besides that, the solution viscosity can rise at high dye concentrations, this can lead to retard mobility of dye molecules which leads to reduce rate of diffusion of dye molecules from bulk solution towards adsorption sites at the surface of the used adsorbent [28].

Effect of pH of MG dye solution on the efficiency of its removal

In order to investigate the effect of pH of dye solution on the efficiency of removal over FeO-NiO (2:1). A series of experiments were performed with keeping all other adsorption conditions constant with variation only pH of dye solution. The effect of pH was screened in the range of (2 – 12). Adjusting of pH of solution was conducted by using hydrochloric acid and sodium hydroxide to adjust pH of dye solution at a desired value. The obtained results are presented in Fig. 11.

From the obtained results, it is clear that, MG dye removal efficiency was increased with increase of pH from pH = 2 to pH = 6 to reach maximum removal efficiency. After this point, dye removal efficiency was reduced steadily from a neutral (7) to a high basic medium (pH=12), with the lowest efficiency seen at a pH of 12. These observations can be related to the effect of pH of solution on the net charge of the surface of the used adsorbent. In this context, the acidity or the basicity of the dye solution would effect on the adsorbent's net charge. In this situation, adsorption is predicted to occur with high efficiency under acidic conditions due to the strong attraction between the adsorbent surface and the negatively charged moieties of the dye molecules. However, the efficiency of dye removal is predicted to be lower in basic media due to the repulsion between the surface of the adsorbent and the dye molecules [29].

Effect of temperature on the efficiency of MG dye removal over FeO-NiO (2:1)

To investigate effect of temperature on the

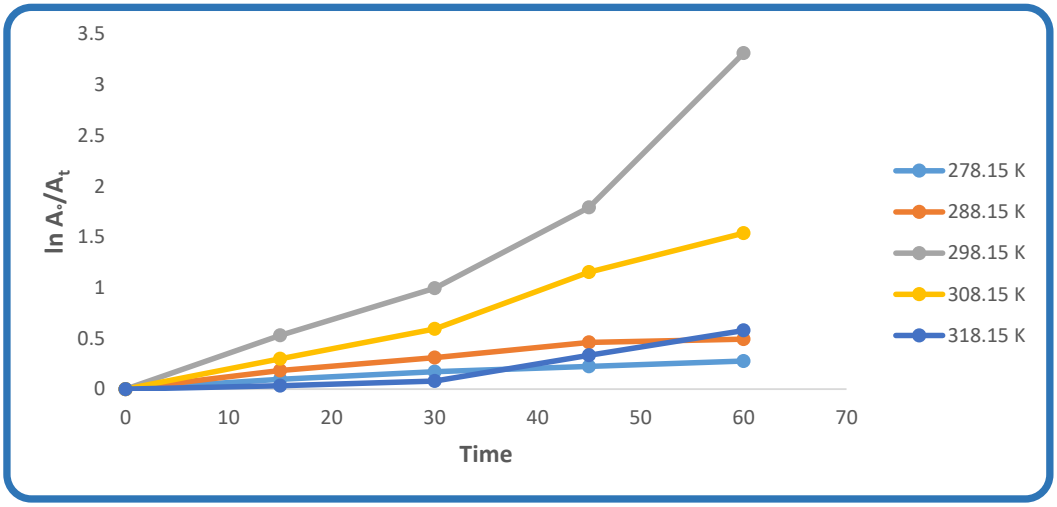

Fig. 13. Evaluating rate constant for adsorption of MG dye over FeO-NiO (2:1) at different temperatures

Table 2. rate constant values for adsorption of MG dye over FeO-NiO (2:1) at different temperatures

Temperature (K)	Reaction rate constant K (min^{-1})
278.15	0.0049
288.15	0.0092
298.15	0.047
308.15	0.0247
318.15	0.0078

efficiency of MG dye removal over the used FeO-NiO (2:1) adsorbent, a series of experiments were conducted in the range of temperature from 5 ℃ to 45℃. All other adsorption conditions were kept constant for each case including using 0.2 g. mass of adsorbent, same dye concentration (20) ppm, and using same adsorption period of one hour for each case. The obtained results are presented in Fig. 12. From the obtained results, it was found that, when the temperature was raised from 5 to 25 ℃, the dye was removed more effectively. It's likely a result of the faster rate at which dye molecules diffuse from the bulk solution into the adsorption sites when the temperature is raised. Additionally, a rise in temperature might decrease the solution's viscosity, resulting in a greater rate of diffusion for the dye molecules [30]. Dye removal effectiveness then decreased with further increases in reaction temperature (over 25 ℃). High temperatures can contribute in increasing kinetics energy of dye molecules and can lead to desorb of dye molecules from adsorption sites into the bulk of solution, this would lead to reduce efficiency of dye adsorption under these circumstances [31].

Rate constant for adsorption of MG dye over FeO-NiO (2:1) was estimated by plotting $\ln A_\infty/At$ as a function of time assuming pseudo first order kinetics, and the obtained results are presented in Fig. 13 and the obtained values of rate constants are presented in Table 2. calculation of reaction rate constant ($Kmin^{-1}$) pseudo first order) of adsorption of MG dye over FeO-NiO (2:1) adsorbent. The magnitude of the slope of the $\ln A_\infty/A_t$ against time graph indicates the reaction rate constant ($K\ min^{-1}$) for the adsorption of MG dye over FeO-NiO (2:1) adsorbent [32].

Calculation of activation energy for adsorption of MG dye over FeO-NiO (2:1)

Activation energy (Ea) for adsorption of MG dye over FeO-NiO (2:1) was calculated by applying

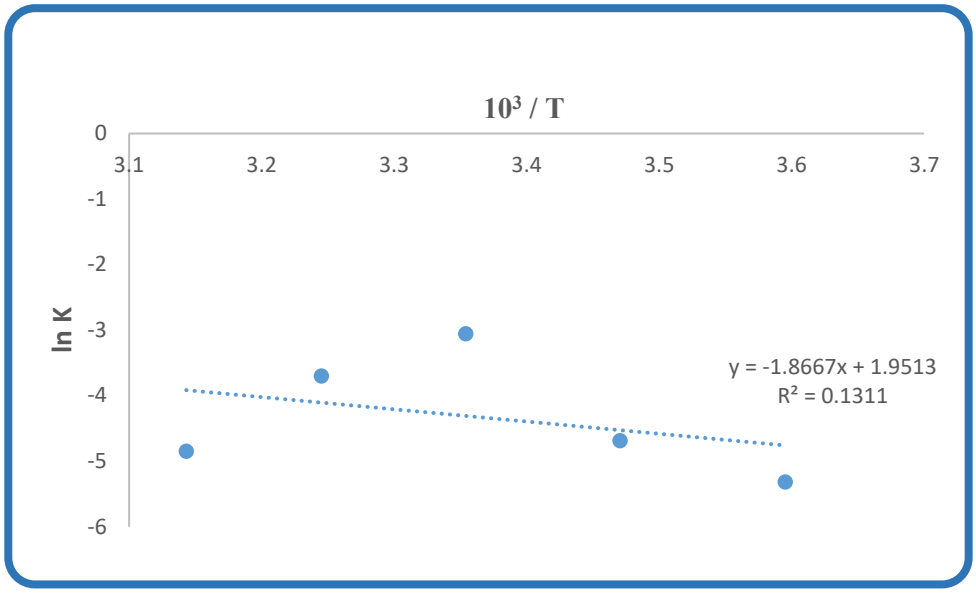

Fig. 14. Arrhenius plot for adsorption of MG dye over FeO-NiO (2:1)

Table 3. Adsorption temperatures and rate constants for adsorption of MG dye over FeO-NiO (2:1)

Temperature (K)	Reaction rate constant K (min^{-1})	1000/T	Ln K
278.15	0.0049	3.595182456	-5.318520074
288.15	0.0092	3.470414715	-4.688551795
298.15	0.047	3.354016435	-3.057607677
308.15	0.0247	3.245172805	-3.700952035
318.15	0.0078	3.14317146	-4.853631545

Arrhenius equation (5). The obtained results are summarized in Table 3 and are plotted in Fig. 14.

$$\ln K = \ln A - \frac{Ea}{RT} \quad (5)$$

Where K reaction rate constant (min^{-1}), A is Arrhenius factor, Ea is activation energy (kJ/mol), R is a universal gas constant = 8.314 (J/mol.K) and T is temperature (K) [33].

From the obtained results, the activation energy that was estimated by applying Arrhenius equation was around 15.5197 KJ/mol. In this case and as the value of the obtained activation energy is considered to be low and it falls in the range of activation of physical energy, its value (5-40 KJ/mol). So that it is worth to suggest physical adsorption occurs in our study, with equilibrium being attained rapidly. In contrast, activation energies for chemical adsorption is much higher (40-800 kJ/mol) [34].

Isothermal study for adsorption of MG dye over FeO-NiO (2:1)

As adsorption processes involve mass transfer through an adhesion process, the adsorbate's charge state is a crucial factor which can affect significantly on adsorption capacity. Therefore, both of the adsorbent and the adsorbate play significant role in the adsorption mechanism. Adsorption isotherm describes the relationship between the adsorbent and adsorbate when the system is in equilibrium at a constant temperature [35]. Adsorption system optimization relies heavily on the examination of isotherm data by fitting to several isotherm models. There are a number of models for adsorption isotherms, however for our investigation, we employed the standard Langmuir and Freundlich models [36].

Langmuir Isotherm

Langmuir adsorption isotherm interest with adsorption that occurs at the uniform surfaces has as its starting point the hypothesis of a uniform adsorbent surface, monolayer adsorbate coverage, and molecular-level activation energy equality. Langmuir adsorption isotherm can be presented in a linear form as follows [37]:

$$\frac{C_e}{q_e} = \frac{1}{K_L\, q_m} + \frac{C_e}{q_m} \quad (6)$$

Where C_e (mg/L), is the equilibrium concentration of the remaining concentration of the adsorbate in the bulk solution, q_e (mg/g) is the amount of adsorbate per unit mass of adsorbent at equilibrium, q_m (mg/g) is the theoretical

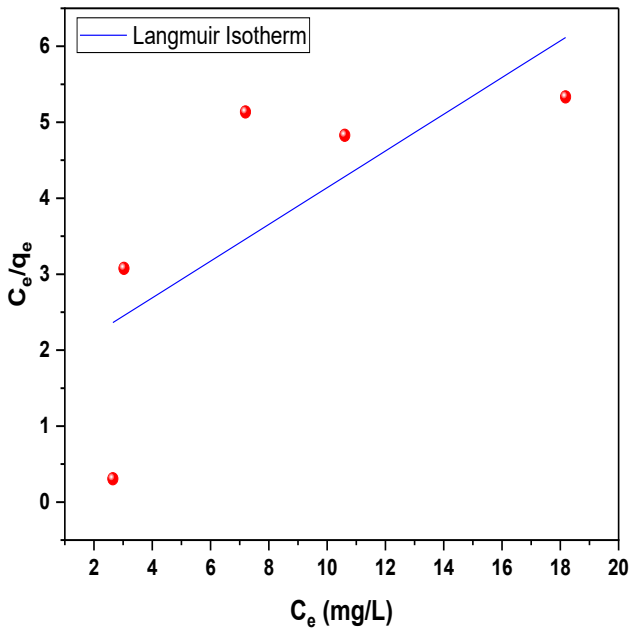

Fig. 15. Langmuir isotherm for adsorption of MG dye over n FeO-NiO (2:1).

saturation capacity of the monolayer, and K_L (L/mg) is Langmuir constant related to the heat of adsorption. Values of q_m and K_L were estimated from the slope and intercept of the linear plot of C_e/q_e against C_e as shown in Fig. 15 and are presented in Table 4.

Freundlich Isotherm

This model can be utilized for multilayers adsorption on heterogeneous surfaces, unlike Langmuir isotherm, which only applies to homogeneous surfaces. This relation can be applied for heterogeneous surfaces [38]. Freundlich relation can be presented as follows;

$$q_e = K_F\, Ce^{1/n} \quad (7)$$

$$\text{Log}\, q_e = \text{Log}\, K_F + \frac{1}{n}\, \text{Log}\, C_e \quad (8)$$

where K_F is a Freundlich isotherm constant, 1/n is the adsorption intensity, C_e is the equilibrium dye concentration, and q_e is the amount of adsorbate per unit mass of adsorbent at equilibrium. Freundlich coefficients n and K_F are acquired from by plotting of (Log q_e) versus (Log C_e). The magnitude of exponent (n) provides an indication of the capacity and favorability of the adsorbate/adsorbent system. When the value of n between 1 and 10, it represents favorable adsorption. When the slope (1/n) ranges between 0 and 1 is a measure of adsorption intensity or surface heterogeneity, becoming more heterogeneous as its value gets closer to zero. While the values less than unity indicate chemisorption process where 1/n over one is an indication of cooperative adsorption [39]. These results are presented in Fig. 16 and are listed Table 4.

From these results, it can be seen that the value

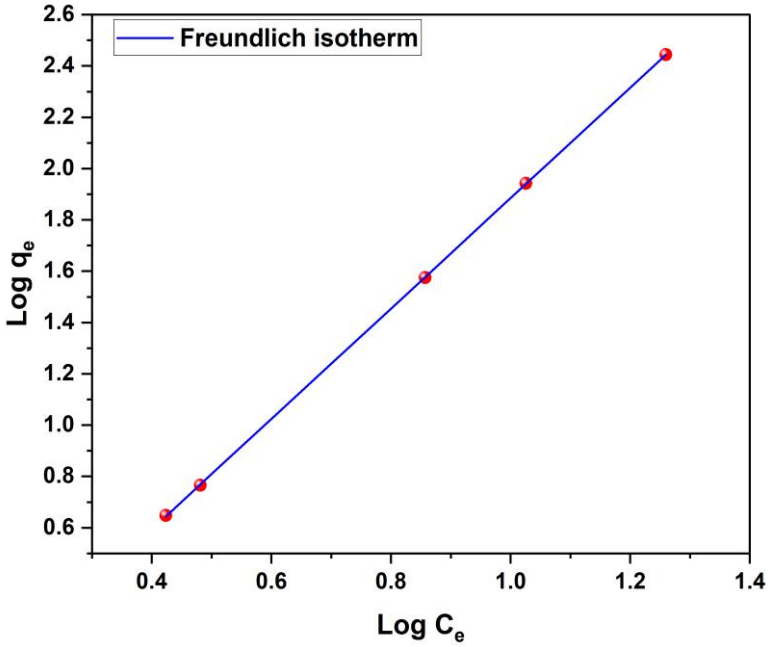

Fig. 16. Freundlich adsorption isotherm for adsorption of MG dye over FeO-NiO (2:1).

Table 4. Langmuir and Freundlich constants for e adsorption of MG dye over FeO-NiO (2:1)

Langmuir isotherm model			Freundlich isotherm model		
q_m (mg/g)	K_L (L/g)	R_L^2	K_F	N	R_F^2
4.1368	0.1404	0.37975	0.5399	0.4645	0.999

of the correlation factor (R^2) that was obtained from Langmuir model is lower than that for Freundlich isotherm. This means that adsorption isotherm in the current study was more fitted with Freundlich model [40].

CONCLUSION

In this study, three composites of iron oxide and nickel oxide were synthesized in three different ratios. Then the activity of these materials was investigated by following removal of MG dye from its aqueous solution by adsorption over these materials. The obtained results showed that, the best removal efficiency was achieved over FeO-NiO (2:1) ratio under using 0.2 g. of the catalyst, 20 ppm of MG dye, 6 pH and 25°C. The optimum removal efficiency was achieved under these conditions was around 96% by adsorption of MG dye over FeO-NiO (2:1) ratio. Also, adsorption isotherm for removal of MG dye by adsorption over FeO-NiO (2:1) was investigated applying both of Langmuir and Freundlich model and the obtained results showed that it was more fitted with Freundlich model and it follows Freundlich adsorption isotherm. Also, the activation energy for adsorption of MG dye over FeO-NiO (2:1) was conducted and it was around 15 kJ/mol., which falls in the range of physical adsorption.

ACKNOWLEDGEMENTS

The authors would like thank University of Babylon, College of Science for their fund and support for this work.

CONFLICT OF INTEREST

The authors declare that there is no conflict of interests regarding the publication of this manuscript.

REFERENCES

1. Mohebi M, Parashkoohi MG, Mohammadi A. A comparison of biofilm and suspension methods in removing heavy metals (chromium) from industrial wastewater with Scenedesmus obliquus and Chlorella vulgaris. Results in Engineering. 2024;24:103397.
2. Gkika DA, Tolkou AK, Evgenidou E, Bikiaris DN, Lambropoulou DA, Mitropoulos AC, et al. Fate and Removal of Microplastics from Industrial Wastewaters. Sustainability. 2023;15(8):6969.
3. Azimi A, Azari A, Rezakazemi M, Ansarpour M. Removal of Heavy Metals from Industrial Wastewaters: A Review. ChemBioEng Reviews. 2017;4(1):37-59.
4. Abdelbasir SM, Shalan AE. An overview of nanomaterials for industrial wastewater treatment. Korean J Chem Eng. 2019;36(8):1209-1225.
5. Adeyemo AA, Adeoye IO, Bello OS. Adsorption of dyes using different types of clay: a review. Applied Water Science. 2015;7(2):543-568.
6. Tan KB, Vakili M, Horri BA, Poh PE, Abdullah AZ, Salamatinia B. Adsorption of dyes by nanomaterials: Recent developments and adsorption mechanisms. Sep Purif Technol. 2015;150:229-242.
7. Sultana M, Rownok MH, Sabrin M, Rahaman MH, Alam SMN. A review on experimental chemically modified activated carbon to enhance dye and heavy metals adsorption. Cleaner Engineering and Technology. 2022;6:100382.
8. Hao R, Xing R, Xu Z, Hou Y, Gao S, Sun S. Synthesis, Functionalization, and Biomedical Applications of Multifunctional Magnetic Nanoparticles. Adv Mater. 2010;22(25):2729-2742.
9. Ali A, Zafar H, Zia M, Ul Haq I, Phull AR, Ali JS, et al. Synthesis, characterization, applications, and challenges of iron oxide nanoparticles. Nanotechnology, science and applications. 2016;9:49-67.
10. Teja AS, Koh P-Y. Synthesis, properties, and applications of magnetic iron oxide nanoparticles. Prog Cryst Growth Charact Mater. 2009;55(1-2):22-45.
11. Raval AR, Kohli HP, Mahadwad OK. Application of emulsion liquid membrane for removal of malachite green dye from aqueous solution: Extraction and stability studies. Chemical Engineering Journal Advances. 2022;12:100398.
12. Photocatalytic Degradation of 1,4-Dioxane and Malachite Green over Zinc Oxide/Cellulose Nanofiber Using UVA/B from Direct Sunlight and a Continuous Flow Reactor. American Chemical Society (ACS).
13. Hashimoto JC, Paschoal JAR, Queiroz SCN, Ferracini VL, Assalin MR, Reyes FGR. A Simple Method for the Determination of Malachite Green and Leucomalachite Green Residues in Fish by a Modified QuEChERS Extraction and LC/MS/MS. J AOAC Int. 2012;95(3):913-922.
14. Bustamante-Torres M, Romero-Fierro D, Estrella-Nuñez J, Arcentales-Vera B, Chichande-Proaño E, Bucio E. Polymeric Composite of Magnetite Iron Oxide Nanoparticles and Their Application in Biomedicine: A Review. Polymers. 2022;14(4):752.
15. Hui BH, Salimi MN. Production of Iron Oxide Nanoparticles by Co-Precipitation method with Optimization Studies of Processing Temperature, pH and Stirring Rate. IOP Conference Series: Materials Science and Engineering. 2020;743(1):012036.
16. Mohammad EJ, Lafta AJ, Kahdim SH. Photocatalytic removal of reactive yellow 145 dye from simulated textile wastewaters over supported (Co, Ni)$_3O_4$/Al_2O_3 co-catalyst. Polish Journal of Chemical Technology. 2016;18(3):1-9.
17. McYotto F, Wei Q, Macharia DK, Huang M, Shen C, Chow CWK. Effect of dye structure on color removal efficiency by coagulation. Chem Eng J. 2021;405:126674.
18. Hjiri M. Highly sensitive NO_2 gas sensor based on hematite nanoparticles synthesized by sol–gel technique. Journal of Materials Science: Materials in Electronics. 2020;31(6):5025-5031.
19. Fazlali F, Mahjoub Ar, Abazari R. A new route for synthesis of spherical NiO nanoparticles via emulsion nano-reactors with enhanced photocatalytic activity. Solid State Sciences. 2015;48:263-269.
20. Schwaminger S, Syhr C, Berensmeier S. Controlled Synthesis of Magnetic Iron Oxide Nanoparticles: Magnetite or Maghemite? Crystals. 2020;10(3):214.

21. Sathya K, Saravanathamizhan R, Baskar G. Ultrasound assisted phytosynthesis of iron oxide nanoparticle. Ultrason Sonochem. 2017;39:446-451.
22. Habibi MH, Fakhri F. Hydrothermal synthesis of nickel iron oxide nano-composite and application as magnetically separable photocatalyst for degradation of Solar Blue G dye. Journal of Materials Science: Materials in Electronics. 2017;28(19):14091-14096.
23. Xie X, Lu C, Xu R, Yang X, Yan L, Su C. Arsenic removal by manganese-doped mesoporous iron oxides from groundwater: Performance and mechanism. Sci Total Environ. 2022;806:150615.
24. Rehman A, Daud A, Warsi MF, Shakir I, Agboola PO, Sarwar MI, et al. Nanostructured maghemite and magnetite and their nanocomposites with graphene oxide for photocatalytic degradation of methylene blue. Materials Chemistry and Physics. 2020;256:123752.
25. Barzinjy AA, Hamad SM, Aydın S, Ahmed MH, Hussain FHS. Green and eco-friendly synthesis of Nickel oxide nanoparticles and its photocatalytic activity for methyl orange degradation. Journal of Materials Science: Materials in Electronics. 2020;31(14):11303-11316.
26. Pillai P, Dharaskar S, Sinha MK, Sillanpää M, Khalid M. Iron oxide nanoparticles modified with ionic liquid as an efficient adsorbent for fluoride removal from groundwater. Environmental Technology and Innovation. 2020;19:100842.
27. Hysna F, Mariana M, Mulana F, Mahidin M, Muchtar S. Physically activated patchouli dregs carbon as a biosorbent for remotion of methylene blue. Materials Today: Proceedings. 2023;87:207-213.
28. Sultana H, Usman M. Surfactant-assisted flocculation for the efficient removal of aqueous dyestuff: A sustainable approach. J Mol Liq. 2023;370:120988.
29. Hojjati-Najafabadi A, Nasr Esfahani P, Davar F, Aminabhavi TM, Vasseghian Y. Adsorptive removal of malachite green using novel GO@ZnO-Ni Fe_2O_4-αAl_2O_3 nanocomposites. Chem Eng J. 2023;471:144485.
30. Dehbi A, Dehmani Y, Omari H, Lammini A, Elazhari K, Abdallaoui A. Hematite iron oxide nanoparticles (α-Fe_2O_3): Synthesis and modelling adsorption of malachite green. Journal of Environmental Chemical Engineering. 2020;8(1):103394.
31. Alwan SH, Alshamsi HA. In situ synthesis NiO/F-MWCNTs nanocomposite for adsorption of malachite green dye from polluted water. Carbon Letters. 2022;32(4):1073-1084.
32. Abu Elella MH, Goda ES, Gamal H, El-Bahy SM, Nour MA, Yoon KR. Green antimicrobial adsorbent containing grafted xanthan gum/SiO_2 nanocomposites for malachite green dye. Int J Biol Macromol. 2021;191:385-395.
33. Crapse J, Pappireddi N, Gupta M, Shvartsman SY, Wieschaus E, Wühr M. Evaluating the Arrhenius equation for developmental processes. Mol Syst Biol. 2021;17(8):e9895-e9895.
34. Igwegbe CA, Ighalo JO, Onyechi KK, Onukwuli OD. Adsorption of Congo red and malachite green using H_3PO_4 and NaCl-modified activated carbon from rubber (Hevea brasiliensis) seed shells. Sustainable Water Resources Management. 2021;7(4).
35. Debnath S, Das R. Strong adsorption of CV dye by Ni ferrite nanoparticles for waste water purification: Fits well the pseudo second order kinetic and Freundlich isotherm model. Ceram Int. 2023;49(10):16199-16215.
36. Hadi AA, Fairooz NY, Atiyah AJ, Al-Khalaf AKH. Removal of Phenol Dye by $CoFe_2O_4$ -$CdFe_2O_4$ Nanocomposites. IOP Conference Series: Earth and Environmental Science. 2021;722(1):012023.
37. Das P, Debnath A. Fabrication of Mg Fe_2O_4/polyaniline nanocomposite for amputation of methyl red dye from water: Isotherm modeling, kinetic and cost analysis. J Dispersion Sci Technol. 2022;44(14):2587-2598.
38. Kalam S, Abu-Khamsin SA, Kamal MS, Patil S. Surfactant Adsorption Isotherms: A Review. ACS omega. 2021;6(48):32342-32348.
39. Zaheer Z, Al-Asfar A, Aazam ES. Adsorption of methyl red on biogenic Ag@Fe nanocomposite adsorbent: Isotherms, kinetics and mechanisms. J Mol Liq. 2019;283:287-298.
40. Dehbi A, Dehmani Y, Omari H, Lammini A, Elazhari K, Abouarnadasse S, et al. Comparative study of malachite green and phenol adsorption on synthetic hematite iron oxide nanoparticles (α-Fe_2O_3). Surfaces and Interfaces. 2020;21:100637.